AIAA JOURNAL
Vol. 43, No. 3, March 2005

Assimilation of Physical Chemistry Models for Lifetime Analysis of Pressure-Sensitive Paint

Wim Ruyten*
Aerospace Testing Alliance, Arnold Air Force Base, Tennessee 37389-6400

Lifetime analysis techniques from the physical chemistry literature are assimilated for use with lifetime-based, pressure-sensitive-paint (PSP) measurements. Effects of finite pulse duration and residual fluorescence, typically avoided in physical chemistry, are included through the use of an excitation response function. Three models are reviewed and applied to the fluorescence decay of PtTFPP in FIB [Pt(II) mesotetra(pentafluorophenyl)porphine in fluoro-isopropyl-butyl], which is the current industry standard for large-scale PSP testing in the United States. These are the discrete exponential model, the Förster decay model, and the maximum entropy model. It is shown how these models invite the reconstruction of the decay rate distribution of the paint from time-resolved measurements of the fluorescence response. Results of the analysis suggest that the decay-rate distribution (and hence the lifetime spectrum) of the paint is bimodal, with each component obeying a linear Stern–Volmer dependence.

Nomenclature

A	=	area under distribution function, mV/μs
a	=	decay rate in Förster decay model (FDM), μs^{-1}
a_k, a_μ	=	amplitudes in discrete exponential and maximum entropy models (DEM and MEM), mV/μs
b	=	Förster correction to decay rate, $\mu s^{-1/2}$
C	=	apparatus constant, mV cm^3/μs
E	=	MEM entropy function
$G(x)$	=	auxiliary function for FDM
i	=	signal index
k, K	=	index, number of terms in DEM
M	=	number of discretization elements in MEM
N	=	number of data points S_i
n_f	=	ground-state fluorophore density, cm^{-3}
$n_\gamma(\gamma)$	=	scaled distribution function with respect to decay rate, mV
$n'_\gamma(\gamma)$	=	distribution function with respect to decay rate, cm^{-3} μs
P	=	air pressure, psf
$p(t)$	=	normalized excitation pulse shape
$S(t)$, S_i	=	measured fluorescence signal, mV
$S_\delta(t)$	=	fluorescence response for delta-function excitation, mV/μs
S_0	=	amplitude in FDM, mV/μs
$s_\gamma(t;\gamma)$	=	excitation response function with respect to γ, μs
T	=	temperature, °F
t, t_0	=	sampling times, μs
t_p, t_c	=	pulse duration and cycle time, μs
γ	=	fluorescence decay rate in air, μs^{-1}
γ_k, γ_μ	=	fluorescence decay rates in DEM, MEM, μs^{-1}
$\Delta\gamma_\mu$	=	MEM discretization element, μs^{-1}
ε	=	relative rms fit error, %
κ_{SV}	=	bimolecular quenching constant, μs^{-1} Kpsf^{-1}
μ	=	discretization index in MEM
σ_i	=	estimated precision of S_i, mV
τ, τ_0	=	fluorescence lifetimes in air and in vacuum, μs
χ^2	=	to-be-minimized quantity in least-squares fit

Presented as Paper 2004-0880 at the 42nd Aerospace Sciences Meeting, Reno, NV, 5–8 January 2004; received 4 February 2004; revision received 21 September 2004; accepted for publication 22 September 2004.

*Engineer Specialist; wim.ruyten@arnold.af.mil. Associate Fellow AIAA.

I. Introduction

OVER the past decade, significant interest has developed in the use of luminescent paints for aerodynamic testing.[1–3] This is particularly true for the use of pressure-sensitive paints (PSPs), which rely on oxygen quenching of fluorescence to produce a pressure-dependent luminescence signal. To lowest order, this process is described by a Stern–Volmer (SV) relation that expresses the fluorescence decay rate γ in terms of the pressure P as

$$\gamma \equiv 1/\tau = 1/\tau_0 + \kappa_{SV} P \tag{1}$$

Here τ is the lifetime in air and τ_0 is the lifetime in vacuum. Higher-order terms are frequently included in Eq. (1), though their origin is usually not well understood.[4–6]

In most PSP measurements, neither the decay rate γ nor the lifetime τ is measured directly. Instead, a ratio is formed between images at wind-off and wind-on conditions when continuous illumination is used, or between images acquired at separate gates following the illumination pulse in the case of pulsed illumination. These two techniques are referred to as intensity-based PSP and lifetime-based PSP, respectively. In both cases, the signal ratio is expressed as a function of pressure, by means of a Stern–Volmer-type relation. To use this relationship as the basis for a pressure measurement, it is not critical that the nature of the relationship (for example, linear vs nonlinear) be well understood, as long as a suitable calibration can be performed. This approach has been fruitful from the early days of PSP measurements.[7,8]

A longstanding complication in PSP measurements is that the signal ratios depend not only on pressure, but also, to a small extent, on temperature.[9–12] Recent work on lifetime-based PSP suggests that this unwanted temperature dependence can be turned to an advantage by extending the standard two-gate measurement scheme to one that employs three or four gates.[13–16] This allows two signal ratios to be formed. Under suitable conditions, this allows both pressure and temperature (P-T) to be obtained.

Questions remain on how to bring such a P-T measurement scheme to fruition. However, it is clear that the fluorescence response of the paint must not be single exponential: Multiple measurements on a single-exponential decay would merely recover the same γ or τ in different ways, leaving the P-T ambiguity unresolved. As it turns out, nonsingle-exponential fluorescence decay of PSPs appears to be the rule, rather than the exception (see Refs. 9 and 14–16, and Sec. III of the present paper). Even so, most PSP analysis to date has been based on single-exponential behavior.[17–20] This approach

falls short if the optimization of a multigate, lifetime-based measurement scheme is to be approached from fundamental principles. Instead, it is desirable to start out from the known lifetime characteristics of the paint or (in the case of paint development) from the desired paint characteristics. In particular, it is desirable that these lifetime characteristics be cast in the form of a mathematical model that can serve as the basis for optimization of the operational parameters of a lifetime-based PSP system, for derivation of suitable calibration equations and for analysis of PSP measurements in general. Such lifetime analysis models have been in use for some time in physical chemistry and associated fields (chemical physics, analytical chemistry, sol-gel physics, and biophysics). The purpose of this paper is to assimilate some of these models for use with PSP (Sec. II) and (in Sec. III) to demonstrate the use of these models for PtTFPP in FIB [Pt(II) mesotetra(pentafluorophenyl)porphine in fluoro-isopropyl-butyl], which is the current industry standard for PSP testing in the U.S.[1,12,13,20–22]

(Editorial note: This paper is based on Refs. 23 and 24, which contain a significant amount of additional material.)

II. Lifetime Models from Physical Chemistry

In Sec. II.A, the notion of paint as a microheterogeneous system is introduced, leading to a general formulation for the response of such a system to delta-function excitation. In Secs. II.B–II.D, three specific realizations of this general model are described. Section II.E deals with the situation in which the width and repetition rate of the excitation pulse cannot be neglected. Section II.F discusses numerical aspects of the reconstruction of the lifetime spectrum of the paint from a time-resolved measurement of the fluorescence signal.

A. Paint as a Microheterogeneous System

A central notion in the description of quenched fluorophore systems is that not all fluorophore molecules experience the same interaction with the quenching species (in the case of current PSPs, this would be oxygen) and that this heterogeneity exhibits itself on a microscopic scale.[25–29] Such a system can be described by partitioning the fluorophore density n_f with respect to the resulting distribution of decay rates γ as

$$n_f \to \int_0^\infty \frac{\mathrm{d}n_f}{\mathrm{d}\gamma}\,\mathrm{d}\gamma \equiv \int_0^\infty n'_\gamma(\gamma)\,\mathrm{d}\gamma = n_f \tag{2}$$

That is, n_f is replaced by a distribution function $n'_\gamma(\gamma)$ that has n_f as its area. Equivalently, this partitioning can be described with respect to the lifetime τ, where $\tau \equiv 1/\gamma$ (Ref. 23). The fluorescence response of such a system to delta-function excitation can be expressed as the Laplace transform

$$S_\delta(t) = \int_0^\infty n_\gamma(\gamma) e^{-\gamma t}\,\mathrm{d}\gamma \tag{3}$$

where $n_\gamma(\gamma)$ is the distribution function $n'_\gamma(\gamma)$ from Eq. (2), multiplied by a constant:

$$n_\gamma(\gamma) \equiv C n'_\gamma(\gamma) \tag{4}$$

The constant C can be written as the product of the area viewed by the detector, the effective thickness of the sample, the excitation photon flux at the surface, the optical cross section for excitation, the quantum efficiency for population of the fluorescing state, the rate of fluorescence decay, the efficiency of detection of emitted fluorescence photons, the detection time, and the number of excitation pulses over which the signal is integrated.[23] Implicit in Eq. (4) is the assumption that the excitation process is linear. This assumption is discussed in detail in Ref. 23.

From Eqs. (2–4) it follows that the area under the distribution $n_\gamma(\gamma)$ is given by

$$A \equiv \int_0^\infty n_\gamma(\gamma)\,\mathrm{d}\gamma = S_\delta(0) = C n_f \tag{5}$$

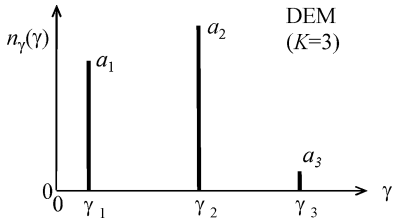

Fig. 1 Illustration of DEM decay rate distribution.

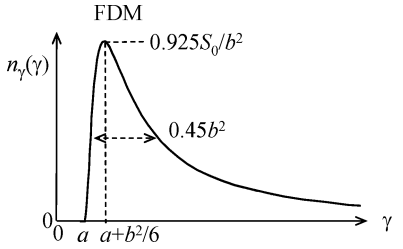

Fig. 2 Illustration of FDM decay rate distribution.

This area should be independent of quenching, a principle that might be paraphrased as "conservation of implied fluorophore density."

B. Discrete Exponential Model

When a single exponential (with to-be-determined amplitude and decay rate) fails to produce a satisfactory fit to fluorescence decay data, it is common practice to add a second, third, and (in rare cases) a fourth term.[9,14,15] This model is known as the discrete exponential model (DEM) and can be expressed as

$$S_{\delta,\mathrm{DEM}}(t) = \sum_{k=1}^{K} a_k \exp(-\gamma_k t) \tag{6}$$

The number of components K can be assigned based on an a priori model (for example, when the components are associated with different fluorophore molecules), or chosen empirically, to get a satisfactory fit to the data. Figure 1 illustrates the associated decay rate distribution for the case $K = 3$. The area under this distribution is given by

$$A_{\mathrm{DEM}} = \sum_{k=1}^{K} a_k \tag{7}$$

C. Förster Decay Model

If the range of interaction distances between fluorophore molecules and quenchers is given by a power-law distribution, the delta-function response of the system can be written as[30–33]

$$S_{\delta,\mathrm{FDM}}(t) = S_0 \exp(-at - bt^{\frac{1}{2}}) \tag{8}$$

where S_0 is the peak signal, a is the Stern–Volmer quenching rate from Eq. (1) with $a = \gamma = 1/\tau$, and b is a measure of the heterogeneity of the quenching process. The exponent $\frac{1}{2}$ in Eq. (8) results for a three-dimensional environment. Exponents $\frac{1}{3}$ and $\frac{1}{6}$ apply to two dimensions and one dimension, respectively.[33] Sometimes, the exponent itself is used as a fitting coefficient.[34] Of particular interest to PSP research is work by Draxler et al.[31] and Draxler and Lippitsch,[32] who found that oxygen-quenching of Ru(dpp) in a series of polymers (i.e., a PSP-like system) could be described better by the Förster decay model (FDM) from Eq. (8) than by the DEM from Eq. (6).

Taking the inverse Laplace transform of Eq. (8), it follows that the associated Förster decay rate distribution is given by[35]

$$n_\gamma(\gamma) = \left(4S_0/\sqrt{\pi}b^2\right) G\left(b/2\sqrt{\gamma - a}\right) \tag{9}$$

where $G(x) \equiv x^3 \exp(-x^2)$ and $n_\gamma(\gamma) = 0$ for $\gamma \le a$. Figure 2 illustrates this distribution, which peaks at $\gamma = a + b^2/6$, has an approximate height $0.925S_0/b^2$, and an approximate full width at

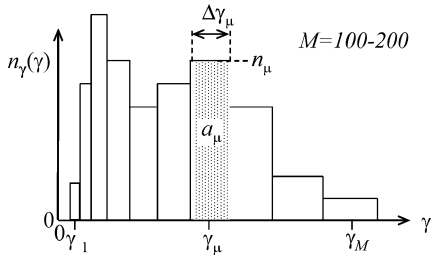

Fig. 3 Illustration of MEM decay rate distribution.

half-maximum given by $0.45b^2$. The area under this distribution, defined by Eq. (5), is precisely equal to the amplitude S_0, that is, $A_{\mathrm{FDM}} = S_0$.

D. Maximum Entropy Model

A model that is formally equivalent to the DEM is one in which the decay rate distribution $n_\gamma(\gamma)$ is represented by a histogram of preselected decay rates γ_μ, with bin widths $\Delta\gamma_\mu$ and to-be-determined bin areas a_μ (Fig. 3).

The delta-function response of such a system can be written as [compare Eq. (6)]:

$$S_{\delta,\mathrm{MEM}}(t) = \sum_{\mu=1}^{M} a_\mu \exp(-\gamma_\mu t) \tag{10}$$

where M is the number of bins in the histogram. Typical values of M are in the range 100–200. Fitting Eq. (10) to a measured fluorescence response is a linear problem (because the γ_μ values are preselected) but one that is highly ill conditioned.[27,35–37] To obtain bin areas a_μ that are physically realistic (not negative and not strongly oscillatory), it is necessary to impose a constraint. In the maximum entropy model (MEM), this constraint is taken to be the Shannon–Jaynes entropy[35–43]

$$E \equiv -\sum_{\mu=1}^{M} \left(\frac{a_\mu}{A}\right) \ell_n \left(\frac{a_\mu}{A}\right) \tag{11}$$

where A is the actual or estimated area under the distribution, given by [compare Eq. (7) for the DEM]

$$A_{\mathrm{MEM}} = \sum_{\mu=1}^{M} a_\mu \tag{12}$$

The discretized values of the distribution function $n_\gamma(\gamma)$ are given, in terms of the bin areas a_μ and the bin widths $\Delta\gamma_\mu$, by $n_\gamma(\gamma_\mu) = a_\mu/\Delta\gamma_\mu$.

E. Excitation Response Function

In physical chemistry, lifetime studies of quenched fluorophore systems are typically performed using short-pulsed lasers, so that the assumption of delta-function excitation is satisfied. In PSP studies this might not be the case [for example, when pulsed light-emitting diodes (LEDs) are used as the excitation source]. Moreover, to minimize PSP measurement time the optimum pulse repetition frequency can be such that small amounts of residual fluorescence (from prior pulses) are tolerated. Both of these complications can be accounted for by convolving the presumed delta-function response of the paint [from Eq. (3), (6), (8), or (10)] by the normalized excitation pulse shape $p(t)$ to arrive at the measured signal $S(t)$, according to

$$S(t) = \int_{-\infty}^{t} p(t_0) S_\delta(t - t_0)\, \mathrm{d}t_0 \tag{13}$$

The lower limit of the integral is set to $-\infty$ to indicate that the measured fluorescence response at time t extends over the entire excitation history of the system, including residual fluorescence from prior pulses.

By combining Eqs. (3) and (13), one can write the signal $S(t)$ as

$$S(t) = \int_0^\infty n_\gamma(\gamma) s_\gamma(t;\gamma)\, \mathrm{d}\gamma \tag{14}$$

where $s_\gamma(t;\gamma)$ is the excitation response function (ERF) for monoexponential decay at a rate γ, given by

$$s_\gamma(t;\gamma) \equiv \int_{-\infty}^{t} p(t_0) e^{-\gamma(t-t_0)}\, \mathrm{d}t_0 \tag{15}$$

The ERF can be calculated analytically for simple pulse shapes, pulse trains, and waveforms, including the case of continuous excitation, with $p(t) = 1$ and $s_\gamma(t;\gamma) = 1/\gamma$ (Ref. 23). Alternatively, the ERF must be calculated by numerical convolution if the pulse shape $p(t)$ is measured experimentally and cannot be described adequately by a simple analytical expression.[24]

F. Reconstruction of Decay Rate Distribution from Measured Fluorescence Response

From the foregoing it follows that fitting a measured fluorescence response can be interpreted as reconstructing the underlying distribution of fluorescence decay rates. To do so, assume that the fluorescence response $S(t)$ has been sampled to yield a set of N values for S_i and that the pulse shape $p(t)$ has been measured, so that the ERF from Eq. (15) can be calculated for any desired value of γ. Fitting the preceding lifetime models to the fluorescence response data can then be cast as a least-squares fitting problem, in which the quantity

$$\chi^2 \equiv \sum_{i=1}^{N} \left\{ \frac{\left[S_i - S_i^{(\mathrm{fit})}\right]}{\sigma_i} \right\}^2 \tag{16}$$

is to be minimized. Here $S_i^{(\mathrm{fit})}$ represents the fitted signal value at point i and σ_i is the estimated uncertainty for this point, proportional to the square root of S_i if photon shot noise is assumed.

In the case of the DEM and FDM, standard nonlinear regression can be used to determine optimum values of the fit parameters.[44] In the DEM from Eq. (6), these are the K amplitudes a_k and associated decay rates γ_k; in the FDM, these are the parameters S_0, a, and b from Eq. (8). In the case of the MEM, the to-be-minimized quantity is $\chi^2 + \lambda E$, where χ^2 is given by Eq. (16), E is given by Eq. (11), and λ is a to-be-determined Lagrange multiplier. Because the number of to-be-determined bin areas a_k in Eq. (10) is typically in the range 100–200, a special algorithm is required.[35–43] (The original MEM algorithm was developed for image reconstruction in astrophysics[45] and has since been adapted for lifetime analysis.[36])

Years of research in physical chemistry (beginning with a seminal paper by James and Ware[46]) have made it clear that it can be difficult to select, on the basis of the magnitude of fitted residuals alone, the best model for a particular system. For example, even if the true dynamics are given by a Förster model, a two-component DEM can give a good fit to the data.[23,31] For this reason, it is desirable to consider not only the magnitude of the residuals, but also the behavior of the fitted parameters as a function of quencher density. This is illustrated in Sec. III.

III. Lifetime Analysis of PtTFPP in FIB

In this section, the theory from Sec. II is applied to fluorescence decay measurements on the pressure-sensitive paint PtTFPP in FIB, which was developed at the University of Washington (Ref. 47; see also following three papers in same issue) and is marketed by Innovative Scientific Solutions, Inc.

A. Experimental

Painted aluminum coupons were mounted in a calibration chamber in which air pressure and sample temperature were precisely controlled. Shop air with a specified dew point of -50°F was used to avoid complications caused by humidity effects. Samples were illuminated at a 45-deg angle by a commercial array of blue LEDs

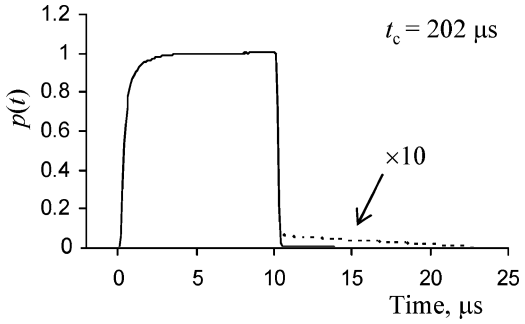

Fig. 4 Normalized illumination pulse shape.

with peak emission at 465 nm, resulting in excitation of the PtTFPP Soret band. The illumination level was held constant to better than 1% over the course of the measurements. Fluorescence from the triplet state, filtered at 650 nm using a 40-nm FWHM custom bandpass filter with 70% transmission, was measured by a fast photomultiplier tube (PMT). The observation direction was also at a 45-deg angle to the sample normals, opposite from the incident light direction.

The LED source was pulsed at 4.95 kHz, giving a train of nearly square light pulses spaced at 202 μs, each with a duration of approximately 10 μs. Output from the PMT was sampled at 0.1-μs intervals from -0.5 μs to about $+100$ μs relative to the trigger input, resulting in 1002 samples per curve. Curves were summed over 100 pulses using a digital oscilloscope. Preprocessing of the data was performed to subtract a baseline value and to determine the precise start of the optical pulse. Calibrations were carried out over a matrix of 25 pressures (from 20 to 2100 psf), each at 10 temperatures in the range 40–120°F.

Figure 4 shows the measured optical pulse shape $p(t)$, which has a rise time of about 0.5 μs and is followed by a small-amplitude tail (0.6% of peak signal) that extends about 13 μs beyond the main cutoff.

Figure 5 shows the measured fluorescence signal $S(t)$ for several pressures at room temperature. Data are plotted on both a linear and a log scale. From the decay part of the fluorescence in Fig. 5b, it is evident that the fluorescence response is not single exponential. Close examination of the data at the lowest pressures (i.e., the data with the longest lifetimes) also reveals the effect of residual fluorescence from pulses prior to the trigger pulse, with a maximum relative contribution of four percent of the peak signal (see Fig. 3 in Ref. 24).

B. Data Analysis

All analysis was based on least-squares fitting of the measured fluorescence response curves, including the excitation phase. Numerical convolution was used to take into account the measured pulse shape and pulse repetition rate.[24] Shot noise was assumed, with relative weights σ_i proportional to the square root of the signals S_i. A Levenberg–Marquardt algorithm (with explicit calculation of derivatives with respect to the fit parameters) was used for the DEM and FDM models. The MEM algorithm was adapted from Ref. 43, with some insights gleaned from Refs. 36 and 41. Convergence times for all three models were typically on the order of several seconds per data set on a 750-MHz Pentium-based processor. A simple peak-finding algorithm was used to identify peaks in the MEM distributions and to calculate the partial area fractions under the peaks relative to the total area under the distribution.

Of the three models tested, MEM consistently produced the best fit to the data. This is expected because of the large number of adjustable parameters. Sample fit residuals, as a percentage of the peak signal (i.e., the signal at the end of the excitation pulse), are shown in Fig. 6. Insets also state the average rms fit error ε as a percentage of the peak signal. Clearly, monoexponential decay (DEM-1) fails to fit the data. Differences between the two-component DEM (DEM-2), FDM, and MEM residuals are more subtle, with the MEM residuals showing the least structure.

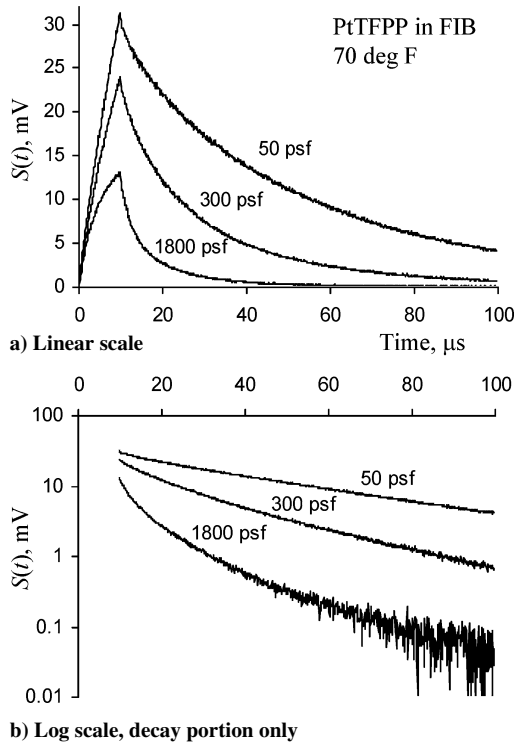

Fig. 5 Selected fluorescence response curves for PtTFPP in FIB at room temperature.

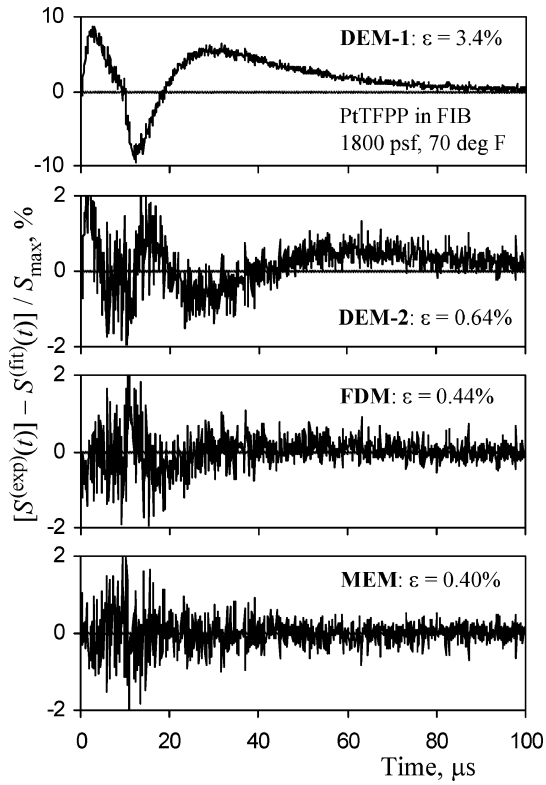

Fig. 6 Fit residuals for data from Fig. 5 for four models.

Figure 7 shows the relative rms error ε vs pressure. As stated, MEM consistently produces the smallest fit errors. Interestingly, for most pressures the three-parameter FDM fits produce lower residuals than the four-parameter DEM fits.

Representative decay rate distributions for the three models are shown in Fig. 8. The vertical axis of Fig. 8 has two sets of units: one for the DEM amplitudes and one for the FDM and MEM distributions. In the FDM case, the spectrum was obtained from Eq. (9)

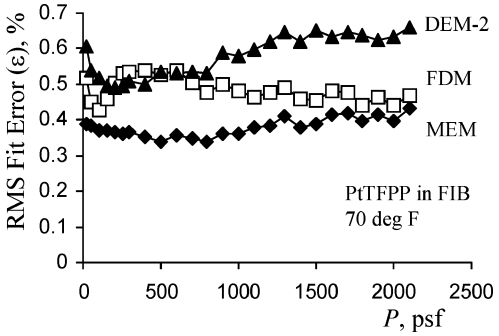

Fig. 7 RMS fit residuals as a function of pressure.

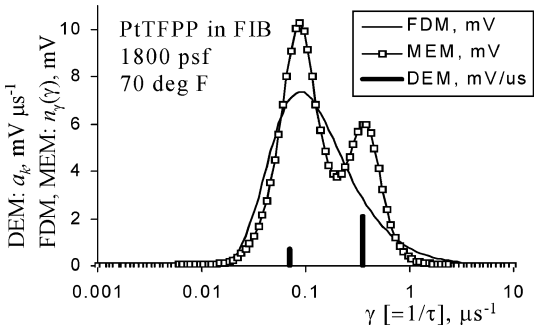

Fig. 8 Implied decay rate distribution for data from Fig. 5.

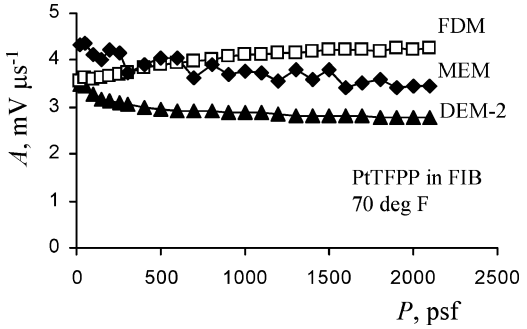

Fig. 9 Areas under distribution function as a function of pressure.

after the data were fitted using Eq. (8). Although the FDM spectrum has only one peak, the MEM and (of course) two-component DEM spectra have two. For some data points, a small third peak was found in the MEM spectrum at small values of γ (Ref. 24). More accurate measurements will be required to confirm that this third peak is not an artifact of the measurement and analysis schemes. Likewise, a three-component DEM fit produced only a marginal improvement over the two-component DEM, with no consistent placement of the third peak as a function of pressure. The two-peaked nature of the MEM spectrum, however, was consistent across all data points, even in cases in which the two peaks were not fully resolved.[24]

Figure 9 shows the areas A under the $n_\gamma(\gamma)$ distributions as a function of pressure for the three models. As argued following Eq. (5), these areas should, ideally, be independent of pressure, a reflection of the fact that the number of fluorophore molecules that participate in the excitation process is constant, regardless of quenching. Mild variations with pressure are found for each of the three models.

Figure 10 shows the FDM parameters a and b from Eq. (8) as functions of pressure. Note the tendency of a toward negative values at large pressures. Figure 11 gives both the MEM and DEM peak positions as functions of pressure. The two sets of peak positions are in reasonable agreement, both suggesting a linear SV dependence as expressed by Eq. (1). Fitted values for the SV intercepts and slopes [expressed in the form of the vacuum lifetimes τ_0 and bimolecular quenching constant κ_{SV} from Eq. (1)] are listed

Table 1 Fitted Stern–Volmer parameters for PtTFPP in FIB at 70°F

Parameter	Value	Slope, %/°F
$\tau_0^{(1)}$, μs	51 ± 4	Unclear
$\tau_0^{(2)}$, μs	21 ± 5	Unclear
$\kappa_{SV}^{(1)}$, μs^{-1} Kpsf^{-1}	0.035 ± 0.004	$+0.11 \pm 0.04$
$\kappa_{SV}^{(2)}$, μs^{-1} Kpsf^{-1}	0.168 ± 0.015	$+0.22 \pm 0.02$

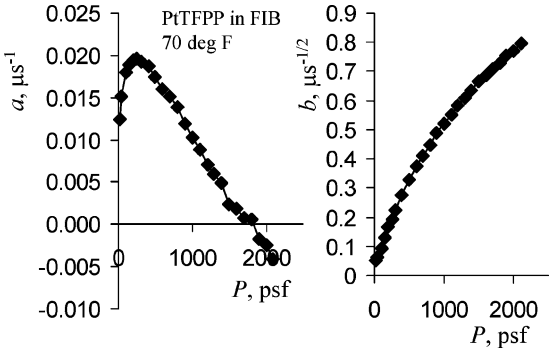

Fig. 10 Förster parameters a and b as a function of pressure.

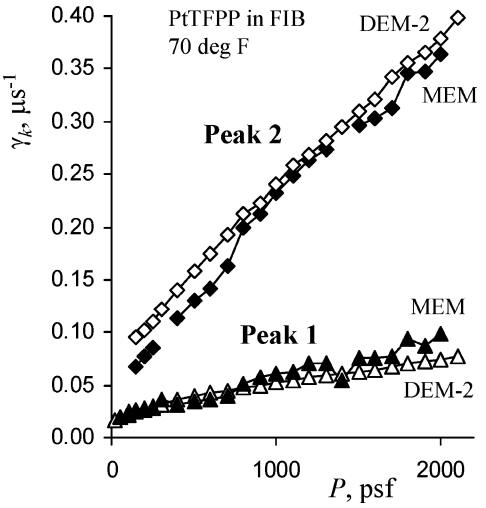

Fig. 11 Stern–Volmer diagram with peak positions vs pressure.

in Table 1, which also lists the estimated uncertainties and fitted temperature sensitivities of these parameters. Finally, Fig. 12 gives the fractional contributions of the two peaks in the DEM and MEM distributions to the total area under the distribution. As is the case in Fig. 11, there is good agreement between the DEM and MEM results.

C. Interpretation of Results

Despite the fact that the FDM tends to produce better fits to the data than does the DEM, it does not appear that the FDM is a physically plausible model for the fluorescence decay of PtTFPP in FIB. In particular, the dependence of the SV parameter a in Fig. 10 is opposite the rise with pressure that is expected and was found by Draxler et al. for the oxygen quenching of Ru(dpp) in a series of polymers.[31] Also, unlike what was found by Draxler et al., the parameter b in Fig. 10 is strongly dependent on quencher density in the present case.

On the other hand, results of MEM analysis appear to confirm that a two-component DEM captures the essence of the fluorescence decay process correctly, even though the DEM does not account for nonzero widths of the peaks in the decay rate distribution. The fact that the MEM produces lower fit residuals than does the DEM indicates that the widths of the MEM peaks have a physical

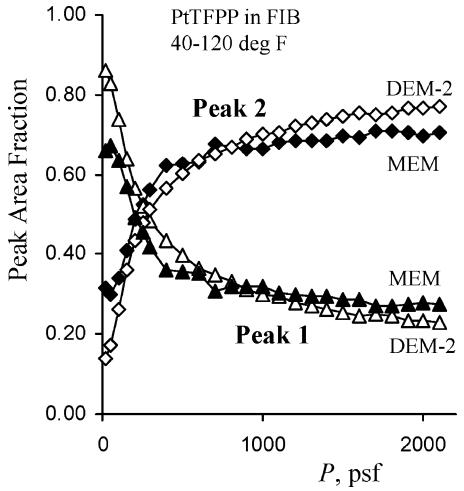

Fig. 12 Peak area fractions associated with Fig. 11.

basis, even though it is known from previous work on MEM that noise on the data leads to broadening of the peaks in the MEM reconstruction.[39,41]

What remains to be explained is why the fractional areas of the two peaks are a strong function of quencher density. This behavior has previously been considered nonphysical from the perspective of a microheterogeneous system, in which each peak is associated with a particular group of fluorophore molecules.[28–31] An alternative explanation is suggested in Ref. 48, which involves a heretofore unknown intermediate state that appears to play a role in the fluorescence decay process. More work will be required to verify the existence of this intermediate state (involving, perhaps, detailed spatial[49] or spectral measurements[50]) and to see if such an intermediate state plays a similar role in other PSP systems.

IV. Conclusions

Three lifetime analysis models from the physical chemistry literature have been reviewed and applied to the fluorescence decay of PtTFPP in FIB, which is the current industry standard for large-scale pressure-sensitive-paint (PSP) testing in the United States. Included in this analysis are two effects that are typically avoided in physical chemistry: the finite width of the excitation pulse and residual fluorescence from prior pulses. Of the three models studied, the maximum entropy model (MEM) produces the best fit to the data and suggests strongly that there are two components in the fluorescence decay. The associated decay rates and relative contribution fractions of these two components are also reproduced by a discrete exponential model (DEM), even though the DEM fit residuals are larger than those of the MEM. A Förster decay model (FDM) does not appear to be a plausible physical model for PtTFPP in FIB, even though it produces lower fit residuals than does the two-component DEM, and even though it has been advocated as an appropriate model for a similar system.[31]

It is anticipated that insights from this work will guide the further development of lifetime-based PSP techniques. In particular, by providing tools for the measurement and modeling of the fluorescence decay dynamics of PSP systems it should become possible to approach the optimization of lifetime-based PSP measurements in a fundamental way. This should be of particular interest to current efforts in which the concept of a two-gate measurement for pressure only is extended to one that encompasses three or four gates, while exploiting the nonsingle-exponential fluorescence dynamics of the paint to measure both pressure and temperature.

Acknowledgments

The research reported herein was performed by the Arnold Engineering Development Center (AEDC), Air Force Materiel Command. Work and analysis for this research were performed by personnel of Aerospace Testing Alliance, operations, maintenance, information management, and support contractor for AEDC. Further reproduction is authorized to satisfy needs of the U.S. Government. The measurements were performed by Marvin Sellers. M. E. Lippitsch of the University of Graz was gracious in supplying supplementary data to Ref. 31. Discussions with J. P. Sullivan of Purdue University are gratefully acknowledged. Partial funding for this work was provided by the Air Force Office of Scientific Research under the Test and Evaluation Program, managed by Neil Glassman.

References

[1]Bell, J. H., Schairer, E. T., Hand, L. A., and Mehta, R. D., "Surface Pressure Measurements Using Luminescent Coatings," *Annual Review of Fluid Mechanics*, Vol. 33, 2001, pp. 155–206.

[2]Liu, T., Campbell, B. T., Burns, S. P., and Sullivan, J. P., "Temperature- and Pressure-Sensitive Paints in Aerodynamics," *Applied Mechanics Review*, Vol. 50, No. 4, 1997, pp. 227–246.

[3]Engler, R. H., Klein, C., and Trinks, O., "Pressure-Sensitive Paint Systems for Pressure Distributions Measurements in Wind Tunnels and Turbomachines," *Measurement Science and Technology*, Vol. 11, No. 7, 2000, pp. 1077–1085.

[4]Carraway, E. R., Demas, J. N., DeGraff, B. A., and Bacon, J. R., "Photophysics and Photochemistry of Oxygen Sensors Based on Luminescent Transition-Metal Complexes," *Analytical Chemistry*, Vol. 63, No. 4, 1991, pp. 337–342.

[5]Mills, A., "Response Characteristics of Optical Sensors for Oxygen: Models Based on a Distribution in τ_0 or k_q," *Analyst*, Vol. 124, No. 9, 1999, pp. 1301–1307.

[6]Mills, A., "Response Characteristics of Optical Sensors for Oxygen: a Model Based on a Distribution in τ_0 and k_q," *Analyst*, Vol. 124, No. 9, 1999, pp. 1309–1314.

[7]Vollan, A., and Alati, L., "A New Optical Measurement System (OPMS)," *Proceedings of the 14th International Congress on Instrumentation in Aerospace Simulation Facilities*, Inst. of Electrical and Electronics Engineers, 1991, pp. 10–16.

[8]Kavandi, J., Callis, J., Gouterman, M., Khalil, G., Wright, D., Burns, D., and McLachlan, B., "Luminescent Barometry in Wind Tunnels," *Review of Scientific Instruments*, Vol. 61, No. 11, 1990, pp. 3340–3347.

[9]Schanze, K. S., Carroll, B. F., Korotkevitch, S., and Morris, M. J., "Temperature Dependence of Pressure Sensitive Paint," *AIAA Journal*, Vol. 35, No. 2, 1997, pp. 306–310.

[10]Coyle, L. M., and Gouterman, M., "Correcting Lifetime Measurements for Temperature," *Sensors and Actuators*, Vol. B61, No. 1–3, 1999, pp. 92–99.

[11]Woodmansee, M. A., and Dutton, J. C., "Treating Temperature-Sensitivity Effects of Pressure-Sensitive Paint Measurements," *Experiments in Fluids*, Vol. 24, No. 2, 1998, pp. 163–174.

[12]Bencic, T. J., "Temperature Correction for Pressure-Sensitive Paint," *NASA Tech Briefs*, Jan. 2000, pp. 50, 51.

[13]Hradil, J., Davis, C., Mongey, K., McDonagh, C., and MacCraith, B. D., "Temperature-Corrected Pressure-Sensitive Paint Measurements Using a Single Camera and a Dual-Lifetime Approach," *Measurement Science and Technology*, Vol. 13, 2002, pp. 1552–1557.

[14]Mitsuo, K., Egami, Y., Suzuki, H., Mizushima, H., and Asai, K., "Development of Lifetime Imaging System for Pressure-Sensitive Paint," AIAA Paper 2002-2909, June 2002.

[15]Mitsuo, K., Asai, K., Takahashi, A., and Mizushima, H., "Advanced Lifetime PSP Imaging System for Simultaneous Pressure and Temperature Measurement," AIAA Paper 2004-2188, June 2004.

[16]Watkins, A. N., Jordan, J. D., Leighty, B. D., Ingram, J. L., and Oglesby, D. M., "Development of Next Generation Lifetime PSP Imaging System," *Proceedings of the 20th International Congress on Instrumentation in Aerospace Simulation Facilities*, Inst. of Electrical and Electronics Engineers, Piscataway, NJ, 2003, pp. 372–377.

[17]Bell, J. H., "Accuracy Limitations of Lifetime-Based Pressure-Sensitive Paint (PSP) Measurements," *International Congress on Instrumentation in Aerospace Simulation Facilities: Record*, Inst. of Electrical and Electronics Engineers, Piscataway, NJ, 2001, pp. 11–16.

[18]Goss, L. P., Trump, D. D., Sarka, B., Lydick, L. N., and Baker, W. M., "Multi-Dimensional Time-Resolved Pressure-Sensitive-Paint Techniques: A Numerical and Experimental Comparison," AIAA Paper 2000-0832, Jan. 2000.

[19]Holmes, J. W., "Analysis of Radiometric, Lifetime, and Fluorescent Lifetime Imaging for Pressure Sensitive Paint," *Aeronautical Journal*, Vol. 102, No. 1014, April 1998, pp. 189–194.

[20]Sellers, M. E., "Application of Pressure Sensitive Paint for Determining Aerodynamic Loads on a Scale Model of the F-16C," AIAA Paper 2000-2528, June 2000.

[21]Baker, W. M., "Recent Experiences with Pressure Sensitive Paint Testing," AIAA Paper 2001-0135, Jan. 2001.

[22]Bencic, T. J., "Calibration of Detection Angle for Full Field Pressure-Sensitive Paint Measurements," AIAA Paper 2001-0307, Jan. 2001.

[23]Ruyten, W., "Assimilation of Physical Chemistry Models for Lifetime Analysis of Pressure-Sensitive Paint," AIAA Paper 2004-0880, Jan. 2004.

[24]Ruyten, W., and Sellers, M., "Lifetime Analysis of the Pressure-Sensitive Paint PtTFPP in FIB," AIAA Paper 2004-0881, Jan. 2004.

[25]Lakowicz, J. R., *Principles of Fluorescence Spectroscopy*, 2nd ed., Kluwer Academic, New York, 1999, Chaps. 4 and 5.

[26]Kalyanasundaram, K., *Photochemistry in Microheterogenous Systems*, Academic Press, Orlando, FL, 1987, Chap. 1.

[27]Liu, Y.-S., and Ware, W. R., "Photophysics of Polycyclic Aromatic Hydrocarbons Adsorbed on Silica Gel Surfaces. 1. Fluorescence Lifetime Distribution Analysis: An Ill-Conditioned Problem," *Journal of Physical Chemistry*, Vol. 97, No. 22, 1993, pp. 5980–5986.

[28]Wang, H., and Harris, J. M., "Origins of Bound-Probe Fluorescence Decay Heterogeneity in the Distribution of Binding Sites on Silica Surfaces," *Journal of Physical Chemistry*, Vol. 99, No. 46, 1995, pp. 16,999–17,009.

[29]James, D. R., Liu, Y.-S., De Mayo, P., and Ware, W. R., "Distributions of Fluorescence Lifetimes: Consequences for the Photophysics of Molecules Adsorbed on Surfaces," *Chemical Physics Letters*, Vol. 120, No. 4–5, 1985, pp. 460–465.

[30]Förster, Th., "Experimentelle und Theoretische Untersuchung des Zwischenmolekularen Übergangs von Elektronenanregungsenergie," *Zeitschrift für Naturforschung*, Vol. 4A, 1949, p. 321.

[31]Draxler, S., Lippitsch, M. E., Klimant, I., Kraus, H., and Wolfbeis, O. S., "Effects of Polymer Matrices on the Time-Resolved Luminescence of a Ruthenium Complex Quenched by Oxygen," *Journal of Physical Chemistry*, Vol. 99, No. 10, 1995, pp. 3162–3167.

[32]Draxler, S., and Lippitsch, M. E., "Lifetime-Based Sensing: Influence of the Microenvironment," *Analytical Chemistry*, Vol. 68, No. 5, 1996, pp. 753–757.

[33]Lakowicz, J. R., *Principles of Fluorescence Spectroscopy*, 2nd ed., Kluwer Academic, New York, 1999, Sec. 4.10.D, Chaps. 13–15.

[34]Wagner, B. D., and Ware, W. R., "Recovery of Fluorescence Lifetime Distributions: Application to Förster Transfer in Rigid and Viscous Media," *Journal of Physical Chemistry*, Vol. 94, No. 9, 1990, pp. 3489–3494.

[35]Siemiarczuk, A., Wagner, B. D., and Ware, W. R., "Comparison of the Maximum Entropy Method and Exponential Series Methods for the Recovery of Distributions of Lifetimes from Fluorescence Lifetime Data," *Journal of Physical Chemistry*, Vol. 94, No. 4, 1990, pp. 1661–1666.

[36]Livesey, A. K., and Brochon, J. C., "Analyzing the Distribution of Decay Constants in Pulse-Fluorimetry Using the Maximum Entropy Method," *Biophysical Journal*, Vol. 52, No. 5, 1987, pp. 693–706.

[37]Brochon, J. C., Livesey, A. K., Pouget, J., and Valeur, B., "Data Analysis in Frequency-Domain Fluorometry by the Maximum Entropy Method—Recovery of Fluorescence Lifetime Distributions," *Chemical Physics Letters*, Vol. 174, No. 5, 1990, pp. 517–522.

[38]Siemiarczuk, A., and Ware, W. R., "A Novel Approach to Analysis of Pyrene Fluorescence Decays in Sodium Dodecylsulfate Micelles in the Presence of Cu^{2+} Ions Based on the Maximum Entropy Method," *Chemical Physics Letters*, Vol. 160, No. 3, 1989, pp. 285–290.

[39]Shaver, J. M., and McGown, L. B., "Maximum Entropy Method for Frequency Domain Fluorescence Lifetime Analysis. 1. Effects of Frequency Range and Random Noise," *Analytical Chemistry*, Vol. 68, No. 1, 1996, pp. 9–17.

[40]McGown, L. B., Hemmingsen, S. L., Shaver, J. M., and Geng, L., "Fluorescence Lifetime Distribution Analysis for Fluorescence Fingerprinting and Characterization," *Applied Spectroscopy*, Vol. 49, No. 1, 1995, pp. 60–66.

[41]Swaminathan, R., and Periasamy, N., "Analysis of Fluorescence Decay by the Maximum Entropy Method: Influence of Noise and Analysis Parameters on the Width of the Distribution of Lifetimes," *Proceedings of the Indian Academy of Sciences*, Vol. 108, No. 1, 1996, pp. 39–49.

[42]Vinogradov, S. A., and Wilson, D. F., "Recursive Maximum Entropy Algorithm and Its Application to the Luminescence Lifetime Distribution Recovery," *Applied Spectroscopy*, Vol. 54, No. 6, 2000, pp. 849–855.

[43]Press, W. H., Teukolsky, S. A., Vetterling, W. T., and Flannery, B. P., *Numerical Recipes in Fortran*, 2nd ed., Cambridge Univ. Press, New York, 1986, Sec. 18.7.

[44]Press, W. H., Teukolsky, S. A., Vetterling, W. T., and Flannery, B. P., *Numerical Recipes in Fortran*, 2nd ed., Cambridge Univ. Press, New York, 1986, Sec. 15.4.

[45]Bryan, R. K., and Skilling, J., "Deconvolution by Maximum Entropy, as Illustrated by Application to the Jet of M87," *Monthly Notices of the Royal Astronomical Society*, Vol. 191, 1980, pp. 69–79.

[46]James, D. R., and Ware, W. R., "A Fallacy in the Interpretation of Fluorescence Decay Parameters," *Chemical Physics Letters*, Vol. 120, No. 4–5, 1985, pp. 455–459.

[47]Puklin, E., Carlson, B., Gouin, S., Costin, C., Green, E., Ponomarev, S., Tanji, H., and Gouterman, M., "Ideality of Pressure-Sensitive Paint. I. Platinum Tetra (Pentafluorophenyl) Porphine in Fluoroacrylic Polymer," *Journal of Applied Polymer Science*, Vol. 77, No. 13, 2000, pp. 2795–2804.

[48]Ruyten, W., "Oxygen Quenching of PtTFPP in FIB Polymer: A Sequential Process?" *Chemical Physics Letters*, Vol. 394, No. 1–3, 2004, pp. 101–104.

[49]Bedlek-Anslow, J. M., Hubner, J. P., Carroll, B. F., and Schanze, K. S., "Micro-Heterogeneous Oxygen Response in Luminescence Sensor Films," *Langmuir*, Vol. 16, No. 24, 2000, pp. 9137–9141.

[50]Bonzagni, N. J., Baker, G. A., Pandey, S., Niemeyer, E. D., and Bright, F. V., "On the Origin of the Heterogeneous Emission from Pyrene Sequestered Within Tetramethylorthosilicate-Based Xerogels: A Decay-Associated Spectra and O_2 Quenching Study," *Journal of Sol-Gel Science and Technology*, Vol. 17, No. 1, 2000, pp. 83–90.

J. Trolinger
Guest Editor